Multidrug resistance-associated protein 4 regulates cAMP-dependent signaling pathways and controls human and rat SMC proliferation

Yassine Sassi,[1] Larissa Lipskaia,[1] Grégoire Vandecasteele,[2] Viacheslav O. Nikolaev,[3] Stéphane N. Hatem,[1] Fleur Cohen Aubart,[1] Frans G. Russel,[4] Nathalie Mougenot,[5] Cédric Vrignaud,[6] Philippe Lechat,[1,6] Anne-Marie Lompré,[1] and Jean-Sébastien Hulot[1,6]

[1]Université Pierre et Marie Curie-Paris 6, INSERM UMR S 621, Paris, France. [2]Université Paris XI, INSERM U769, Chatenay Malabry, France. [3]Rudolf Virchow Center, DFG-Research Center for Experimental Medicine, University of Würzburg, Würzburg, Germany. [4]Department of Pharmacology and Toxicology, Radboud University Nijmegen Medical Centre, Nijmegen, The Netherlands. [5]Université Pierre et Marie Curie-Paris 6, INSERM IFR CMV, Paris, France. [6]Pharmacology Department, Pitié-Salpêtrière University Hospital, Assistance Publique-Hôpitaux de Paris, Paris, France.

The second messengers cAMP and cGMP can be degraded by specific members of the phosphodiesterase superfamily or by active efflux transporters, namely the multidrug resistance-associated proteins (MRPs) MRP4 and MRP5. To determine the role of MRP4 and MRP5 in cell signaling, we studied arterial SMCs, in which the effects of cyclic nucleotide levels on SMC proliferation have been well established. We found that MRP4, but not MRP5, was upregulated during proliferation of isolated human coronary artery SMCs and following injury of rat carotid arteries in vivo. MRP4 inhibition significantly increased intracellular cAMP and cGMP levels and was sufficient to block proliferation and to prevent neointimal growth in injured rat carotid arteries. The antiproliferative effect of MRP4 inhibition was related to PKA/CREB pathway activation. Here we provide what we believe to be the first evidence that MRP4 acts as an independent endogenous regulator of intracellular cyclic nucleotide levels and as a mediator of cAMP-dependent signal transduction to the nucleus. We also identify MRP4 inhibition as a potentially new way of preventing abnormal VSMC proliferation.

Introduction

cAMP and cGMP are second messengers that relay external signals to downstream effector proteins. The most common targets are cAMP-dependent PKA and cGMP-dependent PKG, which regulate a large number of processes by phosphorylating target proteins. In addition to PKA, recent evidence has highlighted a major role for guanine-nucleotide exchange factors for Rap proteins (namely EPAC1 and EPAC2) (1) in mediating cAMP signaling. cAMP and cGMP also act by binding certain ion channels (2). Signaling events triggered by extracellular stimuli arise from an ingenious system of regulation that involves the production and elimination of intracellular cyclic nucleotides. Classically, cyclic nucleotide elimination has been attributed to hydrolysis mediated by cyclic nucleotide phosphodiesterases (PDEs). PDEs constitute a large superfamily of enzymes encoded by several genes with tissue-specific expression of a large number of splice variants (3). In several models, including VSMCs, PDEs have been shown to regulate the amplitude and duration of intracellular cyclic nucleotide signaling (4, 5). For instance, sildenafil, a selective PDE5 inhibitor used to treat human erectile dysfunction by increasing cGMP availability, deactivates multiple signaling pathways associated with cardiac hypertrophy (6) (the calcineurin/NFAT, PI3K/Akt, and ERK1/2 signaling pathways) and prevents the proliferation of VSMCs (7). However, some PDE subfamilies (PDE1 and -4, for instance) (8) are composed of several isoforms that may have specific functional roles. This diversity, adding to the compartmentation of cyclic nucleotide signaling (4, 5), provides a challenge to achieving selective therapeutic effects. Moreover, PDEs may not be the sole regulator of cyclic nucleotide pathways. Indeed, some studies have reported that cAMP and cGMP can exit from the cytosol to the extracellular medium in some specific cell types, including VSMCs (9, 10).

The multidrug resistance-associated protein (MRP) MRP4, also known as ATP-binding cassette transporter family class C4 (*ABCC4*), a member of a large family of transmembrane proteins involved in active transport of substrates out of cells, actively effluxes nucleoside monophosphate analogs from mammalian cells (11). MRP4 and MRP5 (also known as *ABCC5*), another member of the ABCC family, were then shown to function as energy-dependent transporters for cAMP and cGMP (12, 13). MRP4 and MRP5 expression has been reported in several tissues, including smooth muscle (14–16), but their physiological function is unclear. In particular, it is not known whether direct elimination of cyclic nucleotides by these transporters is an additional or an alternative mechanism acting upstream of cyclic nucleotide catabolism.

To delineate the role of MRP4/5 in cyclic nucleotide-dependent biological processes, we used arterial SMCs, as increased cyclic

Nonstandard abbreviations used: Ad-shLuc, adenoviral vector expressing a luciferase shRNA; Ad-shMRP4, adenoviral vector expressing an shRNA against rat Mrp4 mRNA; CFP, cyan fluorescent protein; CREB, cAMP-responsive element binding protein; EC_{50}, 50% of the maximal response to the agonist; FRET, fluorescence responsive energy transfer; hCAEC, human coronary artery endothelial cell; hCASMC, human coronary artery SMC; IBMX, 3-isobutyl-1-methylxanthine; MRP, multidrug resistance-associated protein; PDE, phosphodiesterase; S, supplement; YFP, yellow fluorescent protein.

Conflict of interest: The authors have declared that no conflict of interest exists.

Citation for this article: *J. Clin. Invest.* **118**:2747–2757 (2008). doi:10.1172/JCI35067.

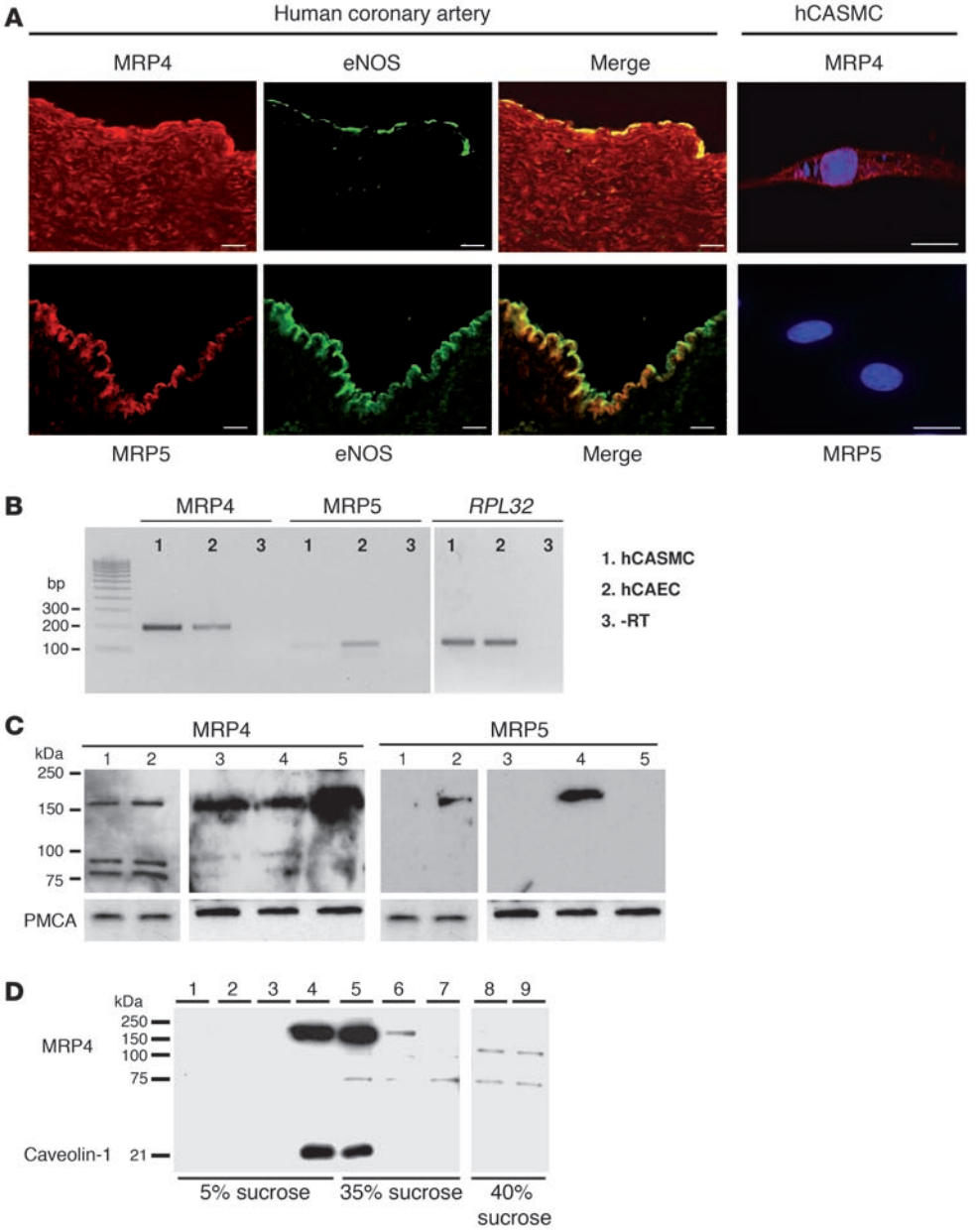

Figure 1
Expression of MRP4 and MRP5 in hCASMCs. (**A**) Immunofluorescence analysis of MRP4 and MRP5 expression (red) on a human coronary artery. eNOS (green) is used as a marker of the endothelium. MRP4 cDNA–transfected hCASMCs were labeled using a polyclonal affinity–purified antibody against MRP4. MRP5 was not detected in hCASMCs. Cells were labeled with DAPI (blue). Scale bars: 20 μm. (**B**) Representative RT-PCR showing detection of MRP4, MRP5, and *RPL32* mRNA in cultured hCASMCs and hCAECs. (**C**) Western blot analysis of MRP4 and MRP5 in total (lane 1) and membrane (lane 2) lysates from hCASMCs and in membranes from wild-type HEK cells (lane 3) and HEK cells stably expressing MRP5 (lane 4) or MRP4 (lane 5). The plasma membrane Ca^{2+} ATPase, PMCA, was used as a loading control. (**D**) Western blot analysis of MRP4 and caveolin-1 expression in hCASMC membranes purified on a discontinuous sucrose gradient, showing that MRP4 is present in caveolin-1–enriched fractions. Lanes are numbered according to the position of fractions from the top to the bottom of the gradient. Lanes 8 and 9 were run on the same gel but were noncontiguous.

nucleotide levels have a well-established role in inducing relaxation of contractile/quiescent SMCs on one hand and in inhibiting proliferation of synthetic/activated SMCs on the other hand (3). We analyzed MRP4/5 expression and function in vitro and in vivo, and we provide what is to our knowledge the first evidence that MRP4 acts as an independent endogenous regulator of cyclic nucleotide intracellular levels, limiting the activation of mediated signal transduction. Our results thus identify MRP4 inhibition as a way of enhancing this signaling pathway.

Results

MRP4 is expressed in coronary artery SMCs. We first examined MRP4 and MRP5 expression in coronary arteries and in isolated primary cultures of human coronary artery SMCs (hCASMCs). In coronary arteries (Figure 1A), MRP4 was mainly detected in medial SMCs and in some luminal endothelial cells, whereas MRP5 was only present in the endothelial layer, visualized by the presence of eNOS. Immunofluorescence analysis of MRP4-transfected hCASMCs showed that the protein is predominantly located on the plasma membrane and in a network around the nucleus. MRP5 could not be detected in hCASMCs (Figure 1A). MRP4 signal was abolished by preincubation with the antigen, and no signal was observed in absence of the primary antibodies (Supplemental Figure 1; supplemental material available online with this article; doi:10.1172/JCI35067DS1), thus showing the specificity of our MRP4-specific antiserum. RT-PCR experiments (Figure 1B) revealed the presence of MRP4 and MRP5 mRNA in hCASMCs and in human coronary artery endothelial cells (hCAECs). However, real-time quantitative PCR analysis showed that MRP4 mRNA level was 6.23 ± 1.74-fold higher ($P < 0.05$) in hCASMCs than in hCAECs, whereas MRP5 was lower in hCASMCs (0.31 ± 0.18-fold compared with hCAECs; $P < 0.05$). At the protein level, the antibody for MRP4 detected the

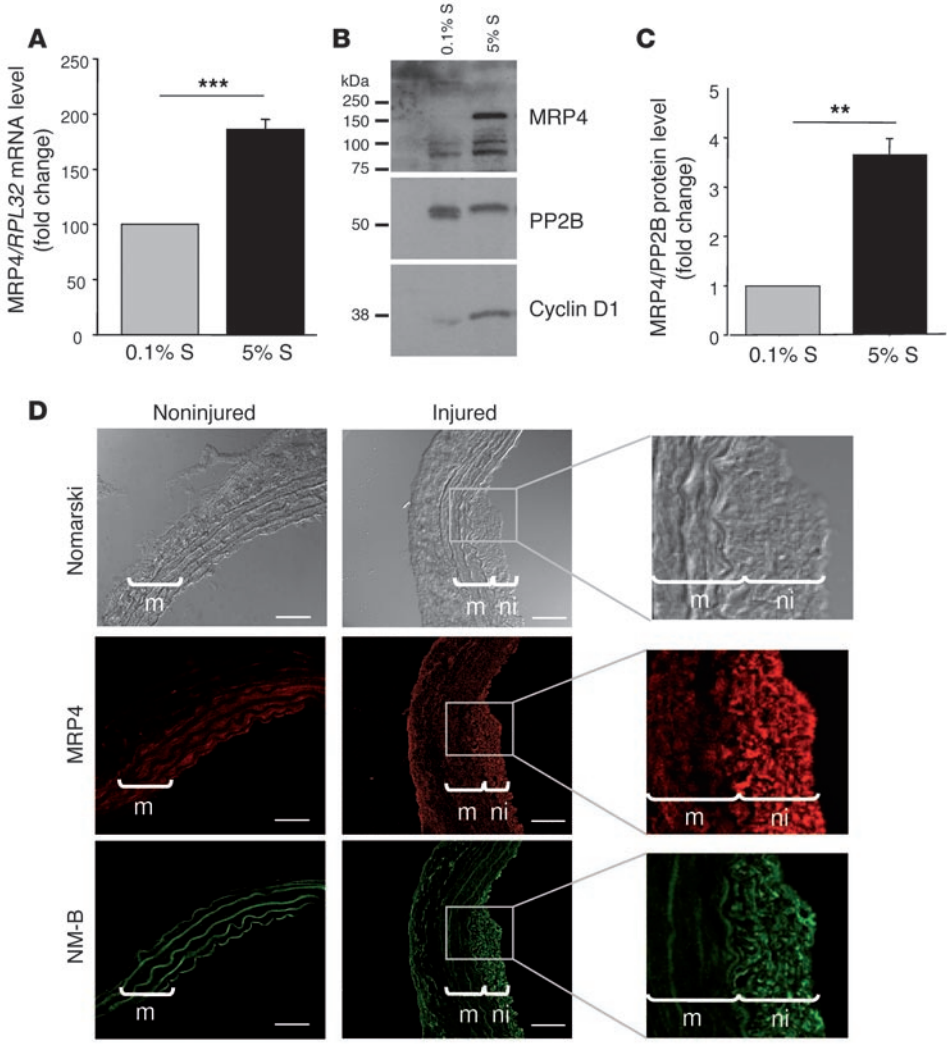

Figure 2
Upregulation of MRP4 in vitro and in vivo in proliferating SMCs. (**A**) MRP4 mRNA level quantified by quantitative real-time PCR in cultured hCASMCs exposed for 72 h to 5% or 0.1% S normalized to the value obtained in 0.1% S. (***$P < 0.001$; $n = 3$) (**B**) Western blot analysis of MRP4 protein expression in the same conditions as described in **A**. PP2B (calcineurin) was used as a loading control and cyclin D1 as a marker of proliferation. (**C**) MRP4 protein level normalized to PP2B (**$P < 0.01$). (**D**) Representative sections of non-injured or balloon-injured rat carotid arteries 14 d after injury. Immunostaining revealed MRP4 expression in the media (m) and predominantly in the neointima (ni). Expression of MRP4 correlated with that of NM-B, a phenotypic marker of SMC proliferation. Scale bars: 50 μm.

expected 160-kDa protein by immunoblotting in both total cell extracts and membrane preparations of hCASMCs, whereas MRP5 protein was detected only in membrane-enriched fractions (Figure 1C). MRP4 was present at similar level in wild-type HEK cells and in HEK cells stably expressing MRP5. Its expression was increased in HEK cells stably expressing MRP4. MRP5 was only detected in HEK cells stably expressing MRP5. As previously reported (17), we also observed 2 low-molecular-weight fragments (of approximately 100 and 75 kDa) using the MRP4 antiserum. We further investigated MRP4 location by separating hCASMC proteins on a 5% to 40% discontinuous sucrose gradient. As shown in Figure 1D, expression of the 160-kDa MRP4 protein was found in low-density fractions also containing the raft-associated protein caveolin-1. The 2 small bands were present in the high-density fractions and may represent MRP4 breakdown products (17).

MRP4 upregulation in proliferating arterial SMCs. MRP4 and MRP5 expression was then examined in quiescent (0.1% supplement [S]) and proliferating hCASMCs stimulated with 5% S by RT-PCR. We observed that the MRP4 mRNA level was increased by 186% ± 9% ($P < 0.001$) in proliferating hCASMCs (Figure 2A), whereas MRP5 mRNA level remained unchanged (94% ± 16%; P = NS; Supplemental Figure 2A). The increase in MRP4 expression was confirmed at the protein level (3.7 ± 0.32-fold higher, $P = 0.01$; Figure 2, B and C). This overexpression correlated with the expression of cyclin D1, a marker of SMC proliferation.

To determine the significance of this increase in vivo, we analyzed the distribution of MRP4 in rat carotid arteries after balloon injury, a well-characterized model of SMC proliferation. As shown in Figure 2D, highly proliferative SMCs in the neointima displayed strong MRP4 protein expression, whereas MRP4 expression in the media was limited. Expression of MRP4 correlated with that of NM-B, a marker of the switch from the quiescent to the proliferative phenotype of SMCs (Figure 2D). Together these data suggest that MRP4 is expressed at a low level in quiescent arterial SMCs and is upregulated in response to proliferative stimuli.

Inhibition of arterial SMC proliferation in vitro by MRP4 siRNA. We first checked the influence of cAMP and cGMP on hCASMC growth in our model. As previously reported, treatment of hCASMCs with the permeant 8-bromo–cAMP (100 μM) or with the adenylate cyclase activator forskolin (5 μM) resulted in significant inhibition of growth supplement–induced proliferation (data not shown). Similar results were obtained with 8-bromo–cGMP (200 μM) and the NO donor SNP (1 mM) (data not shown), confirming the antiproliferative effect of cyclic nucleotides in VSMCs.

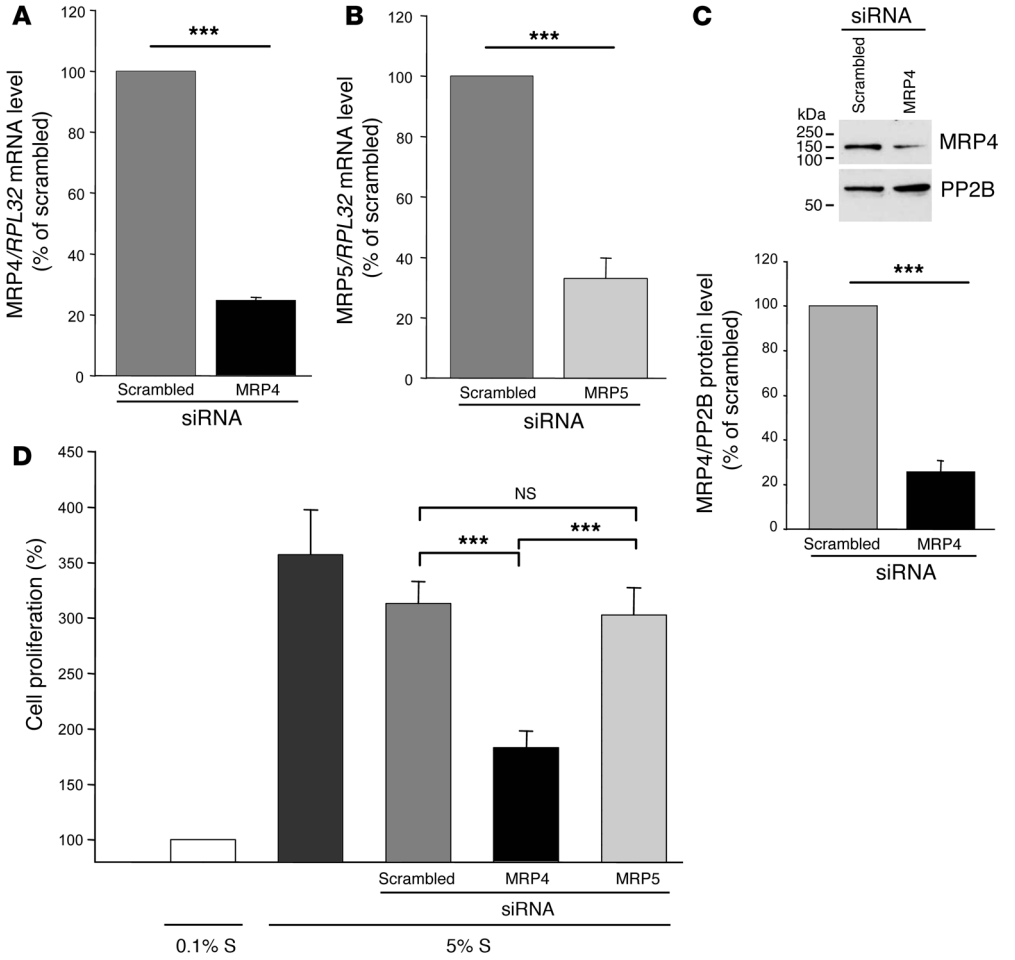

Figure 3
Inhibition of hCASMC proliferation with MRP4 siRNA. Quantitative real-time PCR with gene-specific primers of (**A**) MRP4 and (**B**) MRP5 in hCASMCs transfected for 72 h with MRP4, MRP5, or scrambled siRNA ($n = 3$, $^{***}P < 0.001$). (**C**) Western blot analysis of total lysates of hCASMCs transfected for 72 h with MRP4 siRNA or scrambled siRNA, showing efficient silencing of MRP4. Proteins were incubated with anti-MRP4 or anti-PP2B antibodies. PP2B was used as a loading control. $n = 3$; $P \leq 0.001$. (**D**) Effect of MRP4 and MRP5 siRNAs on hCASMC proliferation (assessed by BrdU incorporation) compared with scrambled siRNA. Proliferation was normalized to the value obtained with 0.1% S. Five experiments were performed in triplicate. $^{***}P \leq 0.001$ for MRP4 compared with scrambled or MRP5 siRNA.

To investigate the role of MRP4 and MRP5 in hCASMCs, we used RNA interference to specifically silence MRP4 and/or MRP5 expression. Transfection of hCASMCs with siRNA against human MRP4 produced, 72 hours later, a decrease in MRP4 mRNA and protein of 75% ± 1% ($P < 0.001$) (Figure 3A) and 74% ± 5.2% ($P < 0.001$) (Figure 3C), respectively, compared with scrambled siRNA. Similar silencing efficiency of MRP5 was obtained with siRNA against human MRP5 (Figure 3B), but MRP4 siRNA had no effect on the level of MRP5 and reciprocally, MRP5 siRNA did not alter the expression of MRP4 at mRNA and protein levels (Supplemental Figure 3).

Stimulation with 5% S increased hCASMC proliferation by 357% ± 41% relative to 0.1% S. We observed that S mix–induced proliferation was significantly lower in hCASMCs transfected with MRP4 siRNA than in those transfected with scrambled siRNA or MRP5 siRNA (increase relative to 0.1% S: 183% ± 15% [MRP4], 313% ± 20% [scrambled], and 303% ± 25% [MRP5], respectively; $P < 0.001$; Figure 4D). Similar results were obtained with alternatively designed and validated MRP4 siRNA (data not shown). MRP4 siRNA did not induce apoptosis of hCASMCs (data not shown). Furthermore, MRP5 siRNA had no effect on hCASMC proliferation (Figure 4D), confirming that specific inhibition of MRP4 is sufficient to block hCASMC growth.

Adenoviral vector expressing shRNA against rat Mrp4 mRNA prevents neointima formation in vivo. To assess the role of MRP4 in preventing VSMC proliferation in vivo, we infected balloon-injured rat carotid arteries with an adenoviral vector expressing shRNA against rat Mrp4 mRNA (Ad-shMRP4; Figure 4A). The capacity of Ad-shMRP4 to silence MRP4 expression was verified in vitro on rat arterial SMC. Seventy-two hours after infection, MRP4 mRNA and protein levels were lower than in cells infected with the same adenoviral vector expressing a luciferase shRNA (Ad-shLuc) (Figure 4, B and C). Ad-shMRP4 had no effect on MRP5 expression (Supplemental Figure 3E).

Two weeks after injury and infection with 10^{11} DNA particles of either Ad-shMRP4 or Ad-shLuc, rats were sacrificed and morphometric analysis of injured carotids was performed on hematoxylin and eosin–stained cross-sections (Figure 4D). The degree of restenosis was determined by measuring intima and media thickness and by calculating the intima/media thickness ratio. These ratios were significantly lower in Ad-shMRP4–infected arteries than in Ad-shLuc–infected arteries ($P < 0.03$; Figure 4E). To confirm adenoviral infection, carotid DNA was extracted from each sample and adenovirus DNA was detected by PCR with specific primers (Figure 4F). These results show that inhibition of MRP4 activity in turn inhibits VSMC proliferation in vitro and balloon injury–induced neointima formation in vivo.

MRP4 inhibition increases cellular cAMP and cGMP levels. Cells transfected with MRP4 siRNA displayed a significant change in cAMP and cGMP levels, with an increase in intracellular and a decrease in extracellular levels. For both cyclic nucleotides, there was a marked

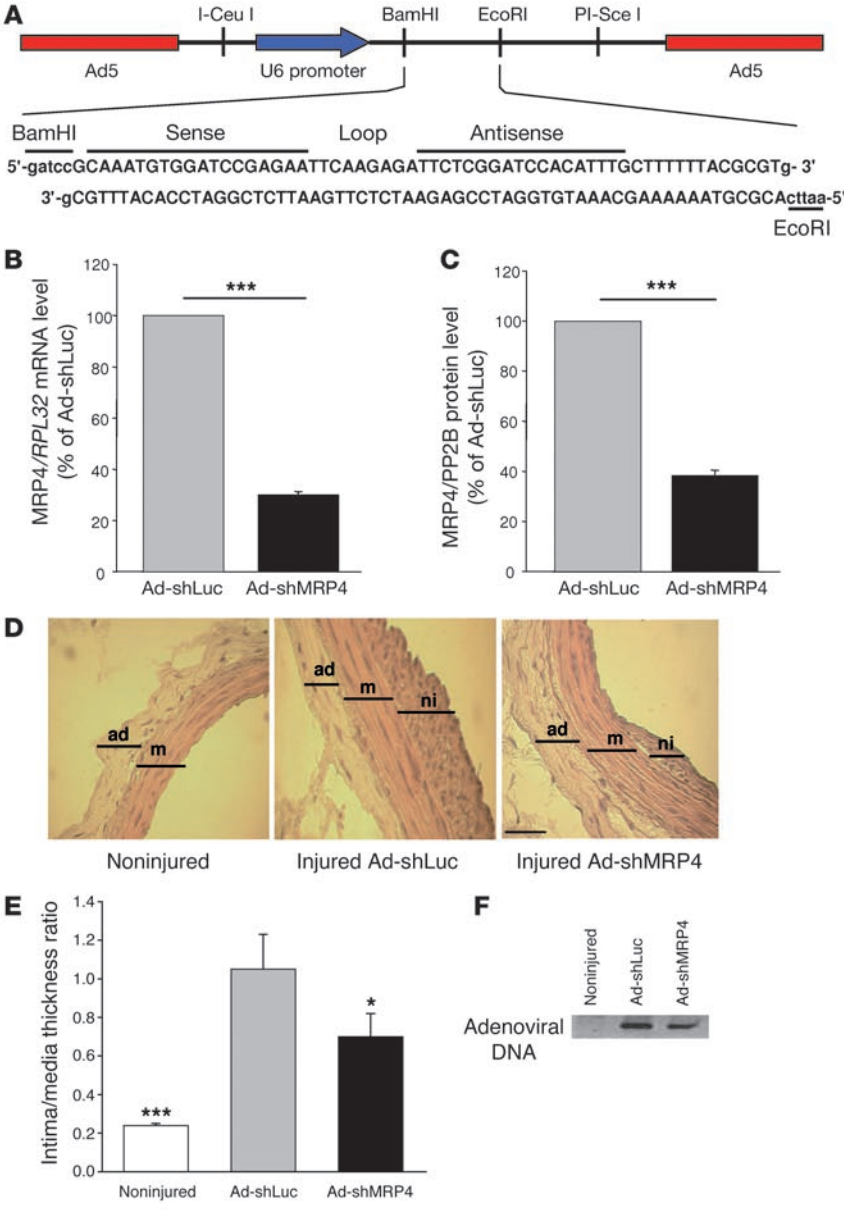

Figure 4
Use of Ad-shMRP4 in vivo. (**A**) Map of the Ad-shMRP4 vector and the MRP4 shRNA sequence. (**B**) Quantitative real-time PCR and (**C**) western blot of rat SMCs transfected for 72 h with Ad-shMRP4 or Ad-shLuc ($n = 3$, $^{***}P < 0.001$). Viruses were used at an MOI of 30. (**D**) Representative hematoxylin and eosin–stained sections of non-injured and injured carotid arteries infected with Ad-shLuc or Ad-shMRP4 14 days after surgery. Scale bar: 50 μm. (**E**) Average intima/media thickness ratios for the above 3 groups ($^{*}P < 0.05$, $^{***}P < 0.001$ compared with Ad-shLuc). ad, adventitia ($n = 5$ for non-injured carotid, $n = 4$ for Ad-shLuc, and $n = 6$ for Ad-shMRP4). (**F**) PCR on carotid arteries. DNA from rat carotids was extracted and adenovirus DNA was detected by PCR.

increase in the intracellular/extracellular ratio (289% ± 12% for cAMP and 230% ± 5% for cGMP, compared with scrambled siRNA), indicating a reduction in cyclic nucleotide efflux from hCASMCs (Figure 5, A and B). A similar increase was observed in hCASMCs treated for 24 hours with the classical PDE inhibitor 3-isobutyl-1-methylxanthine (IBMX) (250% ± 14% for cAMP and 217% ± 11% for cGMP intracellular/extracellular ratios). The increase observed in cells treated with IBMX, however, was significantly higher in hCASMCs transfected with MRP4 siRNA than in hCASMCs transfected with the scrambled siRNA (324% ± 21% for cAMP and 261% ± 17% for cGMP intracellular/extracellular ratios in cells treated with MRP4 siRNA plus IBMX; $P < 0.05$ for both). This indicates that both PDE and MRP4 inhibition result in an independent modification of cyclic nucleotides content. On the contrary, we did not observed any changes in cAMP or cGMP levels in hCASMCs transfected with MRP5 siRNA (Figure 5, A and B). Interestingly, we observed that MRP4 mRNA and protein levels were significantly increased in hCASMCs treated with IBMX (Figure 5, C and D), indicating that MRP4 expression is upregulated in the presence of PDE inhibition.

To further analyze the influence of MRP4 inhibition on cAMP levels, hCASMCs transfected with either MRP4 or scrambled siRNAs were infected with an adenovirus encoding Epac2-camps, a fluorescence resonance energy transfer–based (FRET-based) sensor for real-time cAMP imaging in living cells (18), and were then challenged with increasing concentrations of forskolin. As shown in Figure 6, A and B, application of forskolin at increasing concentrations elicited a rise in cAMP levels reflected by a global increase in the cyan fluorescent protein/yellow fluorescent protein (CFP/YFP) ratio, indicating FRET changes between CFP and YFP. However, stimulation with lower concentrations of forskolin led to a greater change in FRET in hCASMCs transfected with MRP4 siRNA. As shown in Figure 6C, MRP4 silencing resulted in a leftward shift in the forskolin concentration-response curve without affecting the maximal effect of the drug. Hill fitting of the data indicated that the concentration of forskolin providing 50% of maximal cAMP formation was significantly lower in MRP4 siRNA–transfected cells than in scrambled siRNA–transfected cells (50% of the maximal response to the agonist [EC_{50}]: 3.0 ± 0.6 μM versus 9.1 ± 1.1 μM, $P < 0.001$). Such an effect was not observed in MRP5 siRNA–transfected cells (Figure 6C). This result confirms more rapid cAMP availability in response to adenylate cyclase stimulation in cells in which MRP4 is inhibited.

MRP4 inhibition enhances the effect of cAMP on hCASMC proliferation by activating PKA. In keeping with the above results, the concentration-dependent antiproliferative effect of forskolin was significantly enhanced in hCASMCs transfected with MRP4 siRNA compared with those transfected with scrambled siRNA (Figure 7A). In MRP4 siRNA–transfected cells, a small amount of forskolin was sufficient to block hCASMC proliferation: the IC_{50} decreased from 0.79 ± 0.56 μM with scrambled siRNA to 0.11 ± 0.01 μM with MRP4 siRNA. No such effect was seen when the cGMP activator

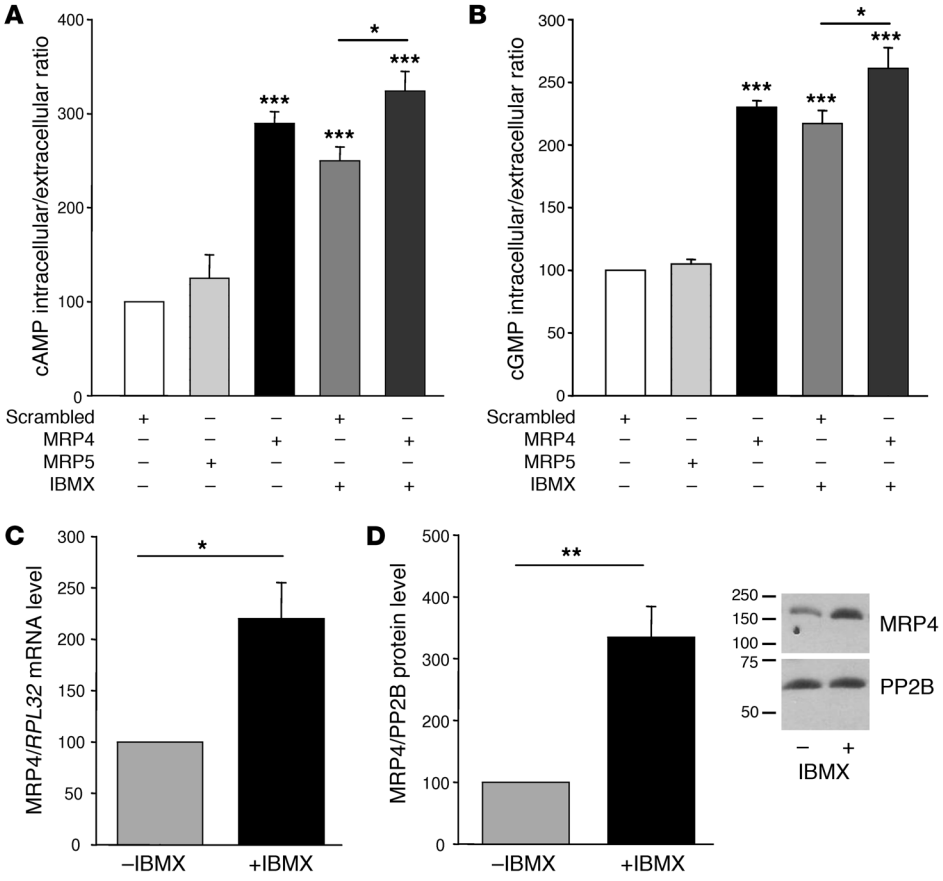

Figure 5
Effect of MRP4 siRNA on cAMP and cGMP cellular levels. Intracellular/extracellular ratios of (**A**) cAMP and (**B**) cGMP, measured with a specific competitive enzyme immunoassay, in hCASMCs transfected with scrambled, MRP5, or MRP4 siRNAs for 72 h and in hCASMCs treated with IBMX (100 μM, 24 h) in the presence or absence of MRP4 siRNA (for 72 h). $n = 3$. (**C**) Relative levels of MRP4 mRNA normalized to *RPL32* mRNA (*$P < 0.05$) and (**D**) MRP4 protein normalized to PP2B in cells untreated or treated with IBMX (100 μM, 24 h). Western blot shows expression of MRP4 and PP2B in hCASMCs untreated or treated with IBMX. *$P < 0.05$, **$P < 0.01$, ***$P < 0.001$.

SNP was used: the IC_{50} was 182 ± 95 μM with scrambled siRNA and 166 ± 90 μM with MRP4 siRNA (Figure 7B).

These results suggest that MRP4 inhibition enhances the effect of cAMP on proliferation more than that of cGMP. We confirmed this by showing that the inhibitory effect of MRP4 siRNA on hCASMC proliferation was completely reversed by inhibition of the cAMP-dependent PKA with an adenoviral vector expressing a PKA inhibitor (Ad-PKI), but not by inhibition of the cGMP-dependent PKG with the pharmacological inhibitor KT5823 (Figure 7C). These results show that MRP4 inhibition enhances the cAMP effect on hCASMC proliferation by activating the PKA-dependent signaling pathway.

Because PKA regulates the activity and phosphorylation of the cAMP-responsive element binding protein (CREB), and because CREB is involved in inhibition of proliferation in SMCs (19), we analyzed the level of phosphorylated CREB (pCREB) in proliferating hCASMCs transfected with scrambled and MRP4 siRNAs. The level of pCREB increased by 329% ± 18.8% ($P = 0.003$) on MRP4 inhibition, whereas the level of total CREB was similar with scrambled and MRP4 siRNA (Figure 8A). We also measured CREB activity in cells transfected with a CRE-luciferase reporter gene. Luciferase activity was significantly higher in cells transfected with MRP4 siRNA than in those transfected with scrambled siRNA (553% ± 25%, $P < 0.01$; Figure 8B). We infer from these results that the antiproliferative effect of MRP4 inhibition involves PKA/CREB pathway activation.

Discussion

To our knowledge, this is the first study to identify MRP4, an energy-dependent efflux pump, as a modulator of signal transduction mediated by cyclic nucleotides and transmitted to the nucleus. Our results indicate that MRP4 acts as a negative regulator that limits the amplitude of cyclic nucleotide signaling in arterial SMCs. This effect was carried by active transmembrane efflux of cyclic nucleotides out of cells, thereby limiting the activation of mediated signal transduction. Specific inhibition of MRP4 in arterial SMCs modified the intracellular content of cyclic nucleotides and markedly enhanced their antiproliferative effect in vitro and in vivo. MRP4 inhibition might therefore have therapeutic implications in vasculoproliferative disorders.

Until now, MRP4 has mainly been viewed as a physiological transporter mediating transmembrane export of endogenous and exogenous glutathione, glucuronate, and sulfate conjugates (20). For instance, MRP4 is expected to be a key actor in the urate elimination pathway (21). MRP4 has also been described as an active transporter of cyclic nucleotides (22–25) and prostaglandins (26). MRP4 may mediate the efflux of antiviral (27, 28) and anticancer (22) purine nucleotide analogs and is involved in storage and release of ADP in platelet-dense granules (29). However, none of these studies identified MRP4 as an upstream regulator of cyclic nucleotide-mediated signaling pathways leading to activation of a new transcription program.

By using RNA interference–mediated silencing of MRP4 in SMC, we detected a significant increase in cAMP and cGMP intracellular levels and a concomitant decrease in extracellular levels in basal conditions. In line with these results, intracellular cAMP availability after stimulation with forskolin, as measured by FRET, was markedly enhanced in cells lacking MRP4 but not

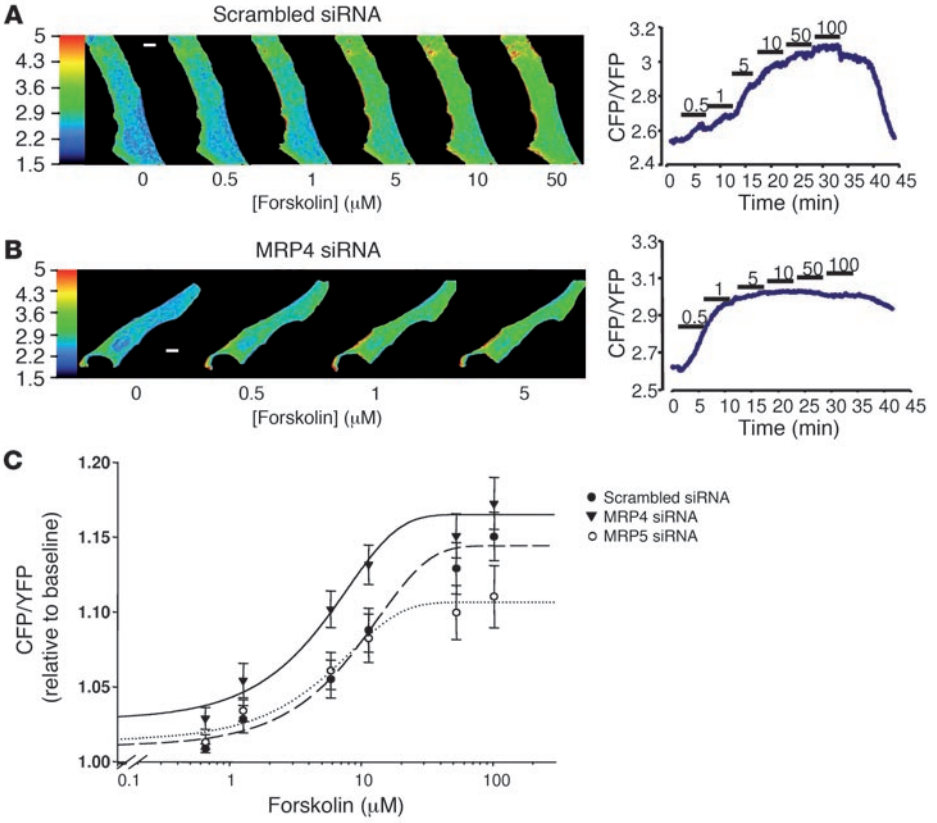

Figure 6

Real-time cAMP imaging in living cells. Effect of forskolin superfused at increasing concentrations (from 0.5 μM to 100 μM) on intracellular cAMP measured with the FRET-based sensor Epac2-camps in 2 representative hCASMCs transfected with (**A**) scrambled or (**B**) MRP4 siRNA. Raw images were obtained upon CFP excitation at 440 ± 20 nm in both cells, and the time course of the corresponding cell average–corrected CFP/YFP ratio are reported. CFP and YFP fluorescence indicated that Epac2-camps was mainly located in the cytosol in both cells. In the scrambled siRNA–transfected cell (**A**), application of 5 μM forskolin increased cAMP, as reflected by the increase in the basal CFP/YFP ratio. In the MRP4 siRNA–transfected cell (**B**), forskolin concentration as low as 0.5 μM significantly increased cAMP. Scale bars: 10 μm. (**C**) Concentration-response curve (logarithmic scale) of FRET measurements in hCASMCs transfected with MRP4 siRNA (triangles, $n = 11$), MRP5 siRNA (open circles, $n = 12$), or scrambled siRNA (filled circles, $n = 18$) and transiently transfected with Epac2-camps. The basal CFP/YFP ratio was similar in the 3 groups of cells. Continuous lines are the fit of the data points to the Hill equation (see Methods). MRP4 RNA interference in hCASMCs resulted in a leftward shift of the forskolin concentration-response curve, as indicated by the significantly different EC_{50} values obtained for the drug in scrambled and MRP4 siRNA groups of experiments.

in those lacking MRP5. These effects were obtained without PDE inhibition, indicating that the intracellular cyclic nucleotide content is determined by 2 independent mechanisms, efflux by MRP4 and catabolism by PDEs. Interestingly, PDE inhibition by IBMX caused a significant upregulation of MRP4 at the mRNA and protein levels. It remains to be determined whether MRP4 inhibition modulated PDE expression and/or activity. However, our results indicate that PDE activity does not counteract the effects induced by MRP4 inhibition. Of note, combined PDE and MRP4 inhibition resulted in a further significant increase in intracellular cyclic nucleotide levels.

Our results point to MRP4 being an alternative or complement to PDEs, ensuring intracellular cyclic nucleotide homeostasis. One of our most intriguing results is that MRP4 inhibition alone was sufficient to modulate intracellular cyclic nucleotide levels and signal transduction. It is now known that PDEs are combined in a complex intracellular spatiotemporal structure (4, 5, 30), controlling specific subcellular pools of cyclic nucleotides. Some PDEs may also translocate from the cytoplasm to the nucleus in proliferating VSMCs (31). In contrast, our observation that MRP4 is localized in caveolin-enriched fractions indicates that MRP4 may exert tighter control over cAMP and cGMP neosynthesis (32, 33). It remains to be seen whether MRP4 quenches cyclic nucleotide production, in contrast to PDEs, which may regulate more specific pools of cyclic nucleotides inside cells.

We observed that inhibition of growth supplement–induced proliferation was associated with an increase in PKA activity. Indeed, adding PKI (a specific inhibitor of PKA) completely reversed the antiproliferative effect of MRP4 inhibition, whereas PKG blockade had no effect. The increase in the phosphorylation and activity of CREB, a nuclear target of the cAMP/PKA signaling pathway (19), is compatible with PKA pathway activation. The cell type–specific antiproliferative effects of cAMP and cGMP are well documented, even if the underlying mechanisms are elusive. In particular, increased cAMP levels are known to inhibit VSMC proliferation in vitro and to reduce neointimal lesion formation after arterial injury in vivo (34–36). Likewise, using the same in vivo model, we observed significant prevention of neointima formation by using Ad-shMRP4. cGMP also inhibits VSMC proliferation in response to mitogens, albeit less potently than cAMP. Expression of a constitutively active PKG has been reported to reduce neointima formation after balloon injury in rats (37). We observed no rescue of the MRP4 inhibitory effect by inhibition of PKG, a key component of the cGMP signaling pathway, raising the possibility that MRP4 inhibition may selectively modulate the cAMP signaling pathway but not the cGMP signaling pathway. However, previous observations suggest that cGMP can act through PKA (38). It was recently shown that the antiproliferative effect of cGMP may involve inhibition of S-phase kinase–associated protein-2 expression through PKA activation (39). It is plausible that cGMP does not directly cross-activate PKA but rather increases cAMP levels by inhibiting the cAMP-hydrolyzing PDE3, as shown in proliferating VSMCs (40). Moreover, intracellular effectors of cAMP and cGMP are compartmentalized in macromolecular complexes, and MRP4 may be an additional partner of these complexes. We found that MRP4 was localized in caveolin-

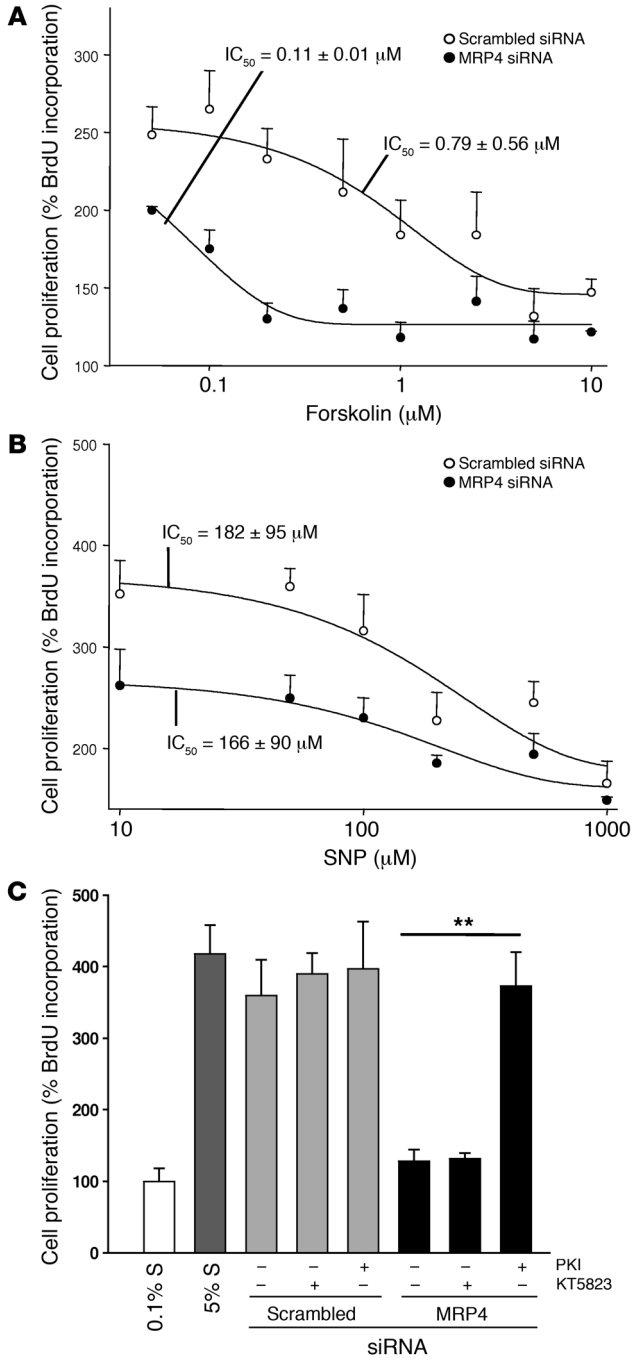

Figure 7
MRP4 inhibition enhances the cAMP effect, but not the cGMP effect, on hCASMC proliferation. Concentration-dependent antiproliferative effect of (**A**) the activator of cAMP-signaling forskolin or (**B**) the activator of cGMP-signaling SNP (n = 5 in triplicate) in cells transfected for 72 h with MRP4 siRNA or scrambled siRNA. (**C**) hCASMC proliferation of cells transfected with MRP4 siRNA or scrambled siRNA in the presence of specific inhibitors of PKA or PKG. The effect of MRP4 inhibition on hCASMC proliferation was reversed in the presence of Ad-PKI but not KT5823 (2 μM, a specific PKG inhibitor) in both cases. n = 3 per group, $^{**}P \leq 0.01$.

enriched membrane fractions. Caveola/lipid rafts are specialized membrane microdomains in which multimolecular complexes of signaling molecules are compartmentalized by interacting with caveolin-1 (41). The MRP4 C-terminal protein sequence contains a consensus PDZ domain-binding motif (42), which suggests that MRP4 could interact tightly with other partners of membrane-signaling complexes. Indeed, in gut epithelial cells, MRP4 is associated with the CFTR Cl channel (25). This indicates that MRP4 may act in specific subcellular domains and thereby modulate an initial activation step of cyclic nucleotide-mediated signal transduction.

This study identifies MRP4 as a regulator of SMC proliferation. MRP4 was weakly expressed in quiescent SMCs, but its expression was induced in vitro and in vivo in proliferative conditions. The factors regulating MRP4 expression are not yet known, but in hepatocytes, MRP4 was shown to be induced by oxidative stress through binding of the oxidative sensor nuclear factor E2-related factor 2 (*Nrf2*) to antioxidant-responsive element sequences in the promoter of *ABCC4* (43). A large body of evidence points to oxidative stress as an important trigger in the complex chain of events leading to atherosclerosis and restenosis (44). Oxidative stress may thus be one of the triggers for increased MRP4 expression in restenosis. We have also shown that IBMX increased MRP4 expression, indicating that MRP4 expression is regulated by the cyclic nucleotides level. Several cAMP-responsive elements are indeed present in the *ABCC4* promoter, but it remains to be determined whether they are functional. Our results suggest that an increased cAMP level induces expression of MRP4, which in turn effluxes the cAMP. MRP4 silencing was associated with an increase in intracellular cAMP level and in CREB activity which regulate the expression of genes involved in the cell cycle. CREB phosphorylation leads to inhibition of cyclin A expression and VSMC proliferation (45). In the short term, oxidative stress induces CREB phosphorylation (46), but in the long term, there is an accelerated entry into cell cycle, accompanied by a significant decrease in CREB content (47). In SMCs, CREB phosphorylation induces immediate early genes such as c-fos (48) in the short term. However, both in vivo and in vitro, the CREB content and phosphorylation are high in quiescent cells and low in the proliferative state (19, 49). Expression of constitutively active CREB decreases both proliferation and chemokinesis (19).

Previous studies have shown MRP5 expression in human SMCs (14, 16), but MRP4 expression was not sought. We detected low levels of MRP5 in VSMCs. It is unlikely that MRP5 acts similarly to MRP4, as we observed no changes in MRP5 expression in VSMC proliferative models and MRP5 silencing affected neither VSMC proliferation nor cyclic nucleotide levels. We cannot, however, exclude the possibility that other MRPs, such as MRP8, are involved in the modulation of cyclic nucleotide-mediated signaling pathways (50).Excessive SMC proliferation is a fundamental process involved in numerous vascular disorders, including atherosclerosis, postangioplasty restenosis, pulmonary arterial hypertension, and vein graft disease (51, 52). Several strategies have been used to modulate cAMP and cGMP levels in these settings, such as adenylyl/guanylate cyclase activation and PDE inhibition. The efficacy of the PDE5A inhibitor sildenafil in the treatment of vasculoproliferative disorders such as primary pulmonary hypertension has been demonstrated (53). Sildenafil itself has been reported to inhibit MRP4 (26); whether its therapeutic efficacy in vascular disorders is linked to PDE5A or MRP4 inhibition (or both) remains to be determined. MRP4 represents an alternative promising

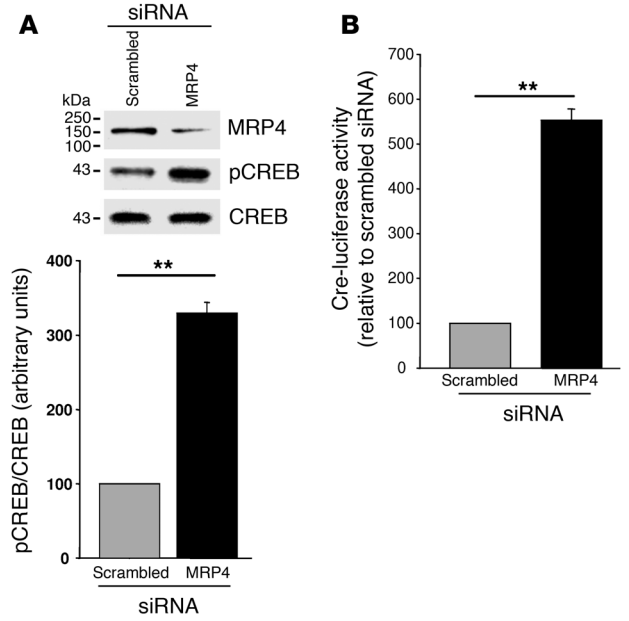

Figure 8

MRP4 inhibition enhances CREB phosphorylation. (**A**) Representative western blot and quantitative evaluation of pCREB in proliferating hCASMCs transfected with MRP4 siRNA or scrambled siRNA ($n = 3$). (**B**) Quantitative evaluation of the activity of the cAMP-responsive element CRE measured with the luciferase reporter CRE-Luc in proliferating hCASMCs transfected with scrambled siRNA or MRP4 siRNA ($n = 3$). $^{**}P < 0.01$.

therapeutic target, as its expression correlates with a pathological response of VSMCs. MRP4 appears to gain functional importance during the proliferative response of SMCs, as supported by the absence of vascular defects in MRP4 knockout mice (54).

In conclusion, our results imply that MRP4 is an important and independent regulator of endogenous cAMP and cGMP levels. MRP4 inhibition might therefore have therapeutic potential by modulating cAMP- and cGMP-mediated signal transduction.

Methods

Reagents. IBMX, 8-bromo–cAMP, 8-bromo–cGMP, SNP, and forskolin were from Sigma-Aldrich. The PKG inhibitor KT5823 was from Calbiochem. The adenovirus PKI was kindly provided by Hazel Lum (University of Illinois, Chicago, Illinois, USA) (55).

All media and sera for culture of human VSMCs were from PromoCell GmbH. Antibiotics were from Invitrogen.

MRP4 and MRP5 stably transfected HEK cells (17) were provided by The Netherlands Cancer Institute.

Human samples and culture of human VSMCs. Fragments of interventricular coronary artery were dissected from explanted human hearts (obtained from the surgical department of the cardiology institute at Hôpital Pitié-Salpêtrière, Paris, France). After removal, the artery segments were immediately immersed in physiological saline solution, placed at 4°C, and used within a few hours. hCASMCs were isolated from the media layer by enzymatic digestion. After dissection, the fragments of media were incubated in SMC basal medium 2 (SMCBM2; PromoCell) with collagenase (CLS2, 50 U/ml; Worthington) and pancreatic elastase (0.25 mg/ml; MP Biomedicals) for 4–6 h at 37°C. After 30-min periods, the suspension was centrifuged at 200 *g* for 3 min and the cells were collected and placed in SMCBM2 + 20% S (10 ng/ml fetal calf serum supplemented with epidermal growth factor, 40 ng/ml basic fibroblast growth factor, 1 mg/ml insulin) (PromoCell). The cells obtained in the first 20-min period were discarded. Those obtained in the other cycles were pooled and cultured in SMCBM2 containing 5% S and antibiotics at 37°C with 5% CO_2. The cells were studied between passages 2 through 6. hCAECs were from Lonza (EGM-2 MV).

Rat carotid artery injury. The animals were treated in accordance with our institutional guidelines. The left external carotid artery of adult male Wistar rats (CERJ) weighing 350 to 400 g was injured as previously described (56). Two weeks after surgery, the carotids were collected and the intima/media thickness ratio was measured on hematoxylin and eosin–stained cross-sections with Lucia software (Nikon). DNA from injured rat carotids was extracted using standard procedures (Puregene DNA Purification Kit; Gentra). Adenovirus expression was then controlled by PCR using a sense primer targeting the inserted expression cassette (5′- TCTTGTGGAAAGGACGAGGA-3′) and an antisense primer located in the adenoviral DNA (5′-ATCAAACGAGTTGGTGCTCA-3′).

Sucrose gradient separation and SDS-PAGE. Protein was isolated by scraping the cells in 2 ml of TNE solution containing (in mM) 20 Tris, 150 NaCl, and 1 EDTA, pH 7.4, to which a cocktail of protease inhibitors (Sigma-Aldrich) was added, and then the cells were homogenized on ice with a glass potter. Triton X-100 was then added to the total protein fraction at a final concentration of 1% in order to solubilize proteins localized in the bulk plasma membranes. Note that all steps of the protein extraction procedure were performed at 4°C, a temperature at which lipid rafts are insoluble in 1% Triton X-100. After 30 min on ice, the protein concentration was determined with the BioRad kit (BioRad Laboratories). Sucrose solution (2 ml, 80%) was placed in a SW41 centrifuge tube (Beckman Coulter), then 2 ml of total extract was placed on the sucrose solution and the preparation was mixed. Sucrose (4 ml, 35%) was gently poured onto the mixture, followed by 4 ml of 5% sucrose. The gradient was then centrifuged for 18 h at 100,000 *g* and 4°C without breaking. Fractions of 1 ml were collected from the top to the bottom of the gradient and kept at –80°C. Each sample fraction was sonicated, then 60 μl was loaded on 12.5% polyacrylamide-SDS gel and analyzed by western blotting.

Western blot analysis and immunofluorescence. Total cell lysates were prepared with a standard protocol (Upstate Biotechnology). Membrane proteins were isolated by scraping the cells in buffer A (5 mmol/l Tris/HCl, 250 mmol/l sucrose, and 0.1 mmol/l EDTA supplemented with a protease inhibitor cocktail; Sigma-Aldrich). The lysate was centrifuged at 10,000 *g* for 10 min at 4°C, and the supernatant was further centrifuged at 100,000 *g* for 1 h at 4°C. The resulting pellet was resuspended in buffer A. Proteins (50 μg) were separated by SDS 12% PAGE, blotted on Hybond-C membranes (Amersham Biosciences), and incubated with various antibodies. The anti-MRP4 antibody has been described elsewhere (23). The other antibodies were anti-MRP5 (Santa Cruz Biotechnology Inc.), anti–caveolin-1 (Abcam), anti–cyclin D1 (BD Biosciences), anti-PP2B (calcineurin; BD Biosciences), anti-CREB (Upstate Biotechnology), anti–pCREB (Upstate Biotechnology), and anti-plasma membrane Ca^{2+} ATPase (Abcam). Immunoreactive proteins were visualized by using an ECL detection system (Amersham Biosciences). Optical density was measured with ImageJ software (NIH). For immunofluorescence, proteins were first incubated with anti-MRP4, anti-MRP5, anti-eNOS (BD Biosciences), or anti–NM-B (Abcam) and visualized by applying secondary antibodies directly conjugated to either Alexa Fluor 546 or Alexa Fluor 488 (Invitrogen). To check for the specificity of the MRP4 antibody, the immunostaining was repeated using a primary antibody incubated overnight with the antigen at 4°C. Under these conditions, no staining could be detected.

Quantitative real-time PCR. Total RNA was prepared with RNeasy Mini kits (Invitrogen), and 1 μg was reverse transcribed using a standard protocol.

One-tenth of the resulting cDNA was amplified by 35 cycles of 30 s at 94°C, 30 s at melting temperature (60°C for MRP4, MRP5, and RPL32), and 30 s at 72°C, followed by a final amplification step at 72°C for 10 min using 1 U of BIOTAQ DNA Polymerase (Bioline) and 200 pmol each of the following primers: human MRP4 sense 5′-TGGTGCAGAAGGGGACTTAC-3′ and antisense 5′-GCTCTCCAGAGCACCATCTT-3′; human MRP5 sense 5′-AGTGCTCTGAAGCCCATCC-3′ and antisense 5′-CCAGAGAAGAAAGCCACGAA-3′; and human RPL32 sense 5′-GCCCAAGATCGTCAAAAAGA-3′ and antisense 5′-GTCAATGCCTCTGGGTTT-3′.

Gene-specific primers were used to amplify mRNA by quantitative PCR on an Mx4000 apparatus (Stratagene) using the Qiagen SYBR Green Master Mix. The specificity of each primer set was monitored by analyzing the dissociation curve. The sample volume was 25 μl, with 1× (final concentration) SYBR Green PCR master mix, 400 nM gene-specific primers, and 5 μl template.

RNA interference. Silencing RNA against human MRP4 was specifically designed by using the academic web-based siRNA design program siSearch (http://sirna.sbc.su.se). The siRNA sequence was designed to target several MRP4-splicing variants (NM_005845, BC041560, AY081219, AF541977, AY133680, AY133679, and AY133678). The sense sequence is 5′-CAGUGUUCUUACACUUCCUTT-3′ and the antisense sequence 5′-AGGAAGUGUAAGAACACUGTT-3′. For the second MRP4 siRNA, the target sequence was 5′-CAAATGTGGATCCGAGAA-3′. siRNA against human MRP5 was from Ambion (catalog no. AM16810). A non-silencing siRNA with no homology with mammalian genes (All Stars Negative Control; Qiagen) was used in parallel (scrambled siRNA).

Cells were transfected with siRNA (50 nM) in S-free medium for 6 h, then the medium was replaced with S-containing medium for a further 66 h. Transfection was performed using Lipofectamine 2000 (Invitrogen) or electroporation using Amaxa Nucleofector technology according to the manufacturer's instructions.

Construction of Ad-shMRP4 and Ad-shLuc. Silencing RNA against rat MRP4 was also specifically designed with the SiSearch program. This siRNA also targeted human MRP4. The shRNA was annealed and ligated via BamHI/EcoRI into pSIREN vector using Knockout RNAi Systems Technology (Clontech). The recombinant pSIREN was then transformed in *E. coli* using Fusion-Blue Competent Cells (Clontech). The fragment was cut out with PI-Sce I/I-Ceu I and inserted into Adeno-X Viral DNA via PI-Sce I/I-Ceu I using Adeno-X Expression System 1 (Clontech). The resulting adenovirus was transfected into HEK293 cells and propagated, thereby generating the adenoviruses designated "Ad-shMRP4" (Figure 5A) and "Ad-shLuc."

To test the efficiency of the adenoviral construct, VSMCs were isolated from the media of the thoracic aorta of male Wistar rats and cultured as previously described (57).

BrdU incorporation in SMCs. Human SMCs were cultured in 96-well tissue culture plates for 3 days in Smooth Muscle Cell Basal Medium 2 (PromoCell) supplemented with 5% S. Medium containing 0.1% S was used for the growth-arrest control. Cells were incubated with pharmacological agents or with siRNA for 72 h in medium containing 5% S. Cell proliferation was measured 3 days after siRNA application following the results on the silencing efficiency, which was measured for a total length of 7 days (Supplemental Figure 3F). BrdU was added for the last 16 h. The plates were washed, and a colorimetric BrdU cell proliferation assay was performed according to the manufacturer's instructions (Roche).

cGMP and cAMP assays. cGMP and cAMP were measured in culture supernatants and lysates of hCASMCs transfected for 72 h with scrambled, MRP5, or MRP4 siRNAs by specific competitive enzyme immunoassay as recommended by the manufacturer (R&D Systems).

Transient transfection and reporter gene assay. Cells were cotransfected with the siRNA (50 nM) and the CRE-luciferase reporter gene plasmid (Stratagene) by electroporation using Amaxa Nucleofector technology according to the manufacturer's instructions. After 6 h the medium was replaced with medium containing 5% S for 66 h. The results are the means of 3 independent experiments performed in triplicate. Luciferase activity was measured using a kit from Promega and was expressed as a percentage of the control value in relative luciferase units.

FRET imaging of cAMP. hCASMCs were transfected with scrambled siRNA or with siRNA against MRP4 (each at 50 nM) in S-free medium for 6 h, then the medium was replaced with S-containing medium. Twenty hours after transfection, the cells were infected with an adenovirus encoding the FRET-based cAMP sensor Epac2-camps at an MOI of 75 pfu/cell. This FRET-based cAMP sensor contained a single cAMP-binding domain of Epac2 fused to YFP and CFP. Upon addition of forskolin, increasing intracellular cAMP concentrations led to a reversible conformational change of Epac2-camps, which resulted in a decrease in FRET between CFP and YFP, leading to an increase in the CFP/YFP ratio (18). Imaging experiments were performed at room temperature after 72 h. Cells were maintained in K^+ Ringer solution containing (in mmol/l): NaCl 121.6, KCl 5.4, $MgCl_2$ 1.8, $CaCl_2$ 1.8, $NaHCO_3$ 4, NaH_2PO_4 0.8, D-glucose 5, sodium pyruvate 5, HEPES 10, adjusted to pH 7.4. Images were captured every 5 s using the ×40 oil immersion objective of a Nikon TE 300 inverted microscope connected to a software-controlled (Metafluor; Molecular Devices) cooled charge-coupled device camera (Sensicam PE; PCO). CFP was excited for 150–300 ms by a xenon lamp (100 W; Nikon) using a 440/20BP filter and a 455LP dichroic mirror. Dual-emission imaging of CFP and YFP was performed using an Optosplit II emission splitter (Cairn Research) equipped with a 495LP dichroic mirror and BP filters 470/30 and 535/30, respectively. Average fluorescence intensity was measured in a region of interest comprising the entire cell. Background was subtracted and YFP intensity was corrected for CFP spillover into the 535-nm channel before calculating the CFP/YFP ratio. Ratio images were obtained with ImageJ software (NIH).

Statistics. All quantitative data are reported as means ± SEM. Statistical analysis was performed with the Prism software package (GraphPad version 3). One-way ANOVA was used to compare each parameter. Post-hoc *t* test comparisons were performed to identify which group differences accounted for significant overall ANOVA results. The concentration-response curve for the effect of forskolin on the normalized CFP/YFP ratio was fitted to the Hill equation $r = E_{max} / (1 + EC_{50} / [\text{forskolin}]^n)$, where EC_{50} is the drug concentration required to produce half-maximal stimulation, E_{max} is the maximal effect, and n is the Hill coefficient. Differences were considered significant at $P < 0.05$.

Acknowledgments

This work was supported by Fondation de France grant 2006005606 and by the Fondation Leducq through the CAERUS network (research agreement 05CVD03 to A.-M. Lompré). Y. Sassi is the recipient of a PhD fellowship from the French Ministère de l'Education Nationale et de la Recherche Scientifique (MENRS). We thank Hazel Lum for providing us with the adenovirus encoding PKI and The Netherlands National Cancer Institute for providing us with the HEK293 cell lines. We thank Claude-Marie Bachelet and Aurélien Dauphin (Plateforme d'imagerie cellulaire Pitié-Salpêtrière) for help in generating the confocal images.

Received for publication January 18, 2008, and accepted in revised form June 11, 2008.

Address correspondence to: Jean-Sébastien Hulot, INSERM U621, Faculté de Médecine Pitié-Salpêtrière, 91 Boulevard de l'Hôpital, 75013 Paris, France. Phone: 33-1-40-77-95-84; Fax: 33-1-40-77-96-45; E-mail: jean-sebastien.hulot@psl.ap-hop-paris.fr.

1. Bos, J.L. 2006. Epac proteins: multi-purpose cAMP targets. *Trends Biochem. Sci.* **31**:680–686.
2. Kaupp, U.B., and Seifert, R. 2002. Cyclic nucleotide-gated ion channels. *Physiol. Rev.* **82**:769–824.
3. Rybalkin, S.D., Yan, C., Bornfeldt, K.E., and Beavo, J.A. 2003. Cyclic GMP phosphodiesterases and regulation of smooth muscle function. *Circ. Res.* **93**:280–291.
4. Fischmeister, R., et al. 2006. Compartmentation of cyclic nucleotide signaling in the heart: the role of cyclic nucleotide phosphodiesterases. *Circ. Res.* **99**:816–828.
5. Houslay, M.D., Baillie, G.S., and Maurice, D.H. 2007. cAMP-Specific phosphodiesterase-4 enzymes in the cardiovascular system: a molecular toolbox for generating compartmentalized cAMP signaling. *Circ. Res.* **100**:950–966.
6. Takimoto, E., et al. 2005. Chronic inhibition of cyclic GMP phosphodiesterase 5A prevents and reverses cardiac hypertrophy. *Nat. Med.* **11**:214–222.
7. Osinski, M.T., Rauch, B.H., and Schror, K. 2001. Antimitogenic actions of organic nitrates are potentiated by sildenafil and mediated via activation of protein kinase A. *Mol. Pharmacol.* **59**:1044–1050.
8. Houslay, M.D., Schafer, P., and Zhang, K.Y. 2005. Keynote review: phosphodiesterase-4 as a therapeutic target. *Drug Discov. Today.* **10**:1503–1519.
9. Hamet, P., Pang, S.C., and Tremblay, J. 1989. Atrial natriuretic factor-induced egression of cyclic guanosine 3′:5′-monophosphate in cultured vascular smooth muscle and endothelial cells. *J. Biol. Chem.* **264**:12364–12369.
10. Kapoor, C.L., and Krishna, G. 1977. Hormone-induced cyclic guanosine monophosphate secretion from guinea pig pancreatic lobules. *Science.* **196**:1003–1005.
11. Sampath, J., et al. 2002. Role of MRP4 and MRP5 in biology and chemotherapy. *AAPS PharmSci.* **4**:E14.
12. Borst, P., de Wolf, C., and van de Wetering, K. 2007. Multidrug resistance-associated proteins 3, 4, and 5. *Pflugers Arch.* **453**:661–673.
13. Ritter, C.A., et al. 2005. Cellular export of drugs and signaling molecules by the ATP-binding cassette transporters MRP4 (ABCC4) and MRP5 (ABCC5). *Drug Metab. Rev.* **37**:253–278.
14. Dazert, P., et al. 2003. Expression and localization of the multidrug resistance protein 5 (MRP5/ABCC5), a cellular export pump for cyclic nucleotides, in human heart. *Am. J. Pathol.* **163**:1567–1577.
15. Mitani, A., Nakahara, T., Sakamoto, K., and Ishii, K. 2003. Expression of multidrug resistance protein 4 and 5 in the porcine coronary and pulmonary arteries. *Eur. J. Pharmacol.* **466**:223–224.
16. Nies, A.T., Spring, H., Thon, W.F., Keppler, D., and Jedlitschky, G. 2002. Immunolocalization of multidrug resistance protein 5 in the human genitourinary system. *J. Urol.* **167**:2271–2275.
17. Wielinga, P.R., et al. 2002. Thiopurine metabolism and identification of the thiopurine metabolites transported by MRP4 and MRP5 overexpressed in human embryonic kidney cells. *Mol. Pharmacol.* **62**:1321–1331.
18. Nikolaev, V.O., Bunemann, M., Hein, L., Hannawacker, A., and Lohse, M.J. 2004. Novel single chain cAMP sensors for receptor-induced signal propagation. *J. Biol. Chem.* **279**:37215–37218.
19. Klemm, D.J., et al. 2001. cAMP response element-binding protein content is a molecular determinant of smooth muscle cell proliferation and migration. *J. Biol. Chem.* **276**:46132–46141.
20. Deeley, R.G., Westlake, C., and Cole, S.P. 2006. Transmembrane transport of endo- and xenobiotics by mammalian ATP-binding cassette multidrug resistance proteins. *Physiol. Rev.* **86**:849–899.
21. Van Aubel, R.A., Smeets, P.H., van den Heuvel, J.J., and Russel, F.G. 2005. Human organic anion transporter MRP4 (ABCC4) is an efflux pump for the purine end metabolite urate with multiple allosteric substrate binding sites. *Am. J. Physiol. Renal Physiol.* **288**:F327–F333.
22. Chen, Z.S., Lee, K., and Kruh, G.D. 2001. Transport of cyclic nucleotides and estradiol 17-beta-D-glucuronide by multidrug resistance protein 4. Resistance to 6-mercaptopurine and 6-thioguanine. *J. Biol. Chem.* **276**:33747–33754.
23. van Aubel, R.A., Smeets, P.H., Peters, J.G., Bindels, R.J., and Russel, F.G. 2002. The MRP4/ABCC4 gene encodes a novel apical organic anion transporter in human kidney proximal tubules: putative efflux pump for urinary cAMP and cGMP. *J. Am. Soc. Nephrol.* **13**:595–603.
24. Wielinga, P.R., et al. 2003. Characterization of the MRP4- and MRP5-mediated transport of cyclic nucleotides from intact cells. *J. Biol. Chem.* **278**:17664–17671.
25. Li, C., et al. 2007. Spatiotemporal Coupling of cAMP Transporter to CFTR Chloride Channel Function in the Gut Epithelia. *Cell.* **131**:940–951.
26. Reid, G., et al. 2003. Characterization of the transport of nucleoside analog drugs by the human multidrug resistance proteins MRP4 and MRP5. *Mol. Pharmacol.* **63**:1094–1103.
27. Schuetz, J.D., et al. 1999. MRP4: A previously unidentified factor in resistance to nucleoside-based antiviral drugs. *Nat. Med.* **5**:1048–1051.
28. Imaoka, T., et al. 2007. Functional involvement of multidrug resistance-associated protein 4 (MRP4/ABCC4) in the renal elimination of the antiviral drugs adefovir and tenofovir. *Mol. Pharmacol.* **71**:619–627.
29. Jedlitschky, G., et al. 2004. The nucleotide transporter MRP4 (ABCC4) is highly expressed in human platelets and present in dense granules, indicating a role in mediator storage. *Blood.* **104**:3603–3610.
30. Dodge-Kafka, K.L., et al. 2005. The protein kinase A anchoring protein mAKAP coordinates two integrated cAMP effector pathways. *Nature.* **437**:574–578.
31. Nagel, D.J., et al. 2006. Role of nuclear Ca2+/calmodulin-stimulated phosphodiesterase 1A in vascular smooth muscle cell growth and survival. *Circ. Res.* **98**:777–784.
32. Ostrom, R.S., et al. 2002. Localization of adenylyl cyclase isoforms and G protein-coupled receptors in vascular smooth muscle cells: expression in caveolin-rich and noncaveolin domains. *Mol. Pharmacol.* **62**:983–992.
33. Linder, A.E., McCluskey, L.P., Cole, K.R., 3rd, Lanning, K.M., and Webb, R.C. 2005. Dynamic association of nitric oxide downstream signaling molecules with endothelial caveolin-1 in rat aorta. *J. Pharmacol. Exp. Ther.* **314**:9–15.
34. Indolfi, C., et al. 1997. Activation of cAMP-PKA signaling in vivo inhibits smooth muscle cell proliferation induced by vascular injury. *Nat. Med.* **3**:775–779.
35. Assender, J.W., Southgate, K.M., Hallett, M.B., and Newby, A.C. 1992. Inhibition of proliferation, but not of Ca2+ mobilization, by cyclic AMP and GMP in rabbit aortic smooth-muscle cells. *Biochem. J.* **288**:527–532.
36. Southgate, K., and Newby, A.C. 1990. Serum-induced proliferation of rabbit aortic smooth muscle cells from the contractile state is inhibited by 8-Br-cAMP but not 8-Br-cGMP. *Atherosclerosis.* **82**:113–123.
37. Sinnaeve, P., et al. 2002. Overexpression of a constitutively active protein kinase G mutant reduces neointima formation and in-stent restenosis. *Circulation.* **105**:2911–2916.
38. Cornwell, T.L., Arnold, E., Boerth, N.J., and Lincoln, T.M. 1994. Inhibition of smooth muscle cell growth by nitric oxide and activation of cAMP-dependent protein kinase by cGMP. *Am. J. Physiol.* **267**:C1405–C1413.
39. Wu, Y.J., Bond, M., Sala-Newby, G.B., and Newby, A.C. 2006. Altered S-phase kinase-associated protein-2 levels are a major mediator of cyclic nucleotide-induced inhibition of vascular smooth muscle cell proliferation. *Circ. Res.* **98**:1141–1150.
40. Aizawa, T., et al. 2003. Role of phosphodiesterase 3 in NO/cGMP-mediated antiinflammatory effects in vascular smooth muscle cells. *Circ. Res.* **93**:406–413.
41. Gratton, J.P., Bernatchez, P., and Sessa, W.C. 2004. Caveolae and caveolins in the cardiovascular system. *Circ. Res.* **94**:1408–1417.
42. Russel, F.G., Masereeuw, R., and van Aubel, R.A. 2002. Molecular aspects of renal anionic drug transport. *Annu. Rev. Physiol.* **64**:563–594.
43. Maher, J.M., et al. 2007. Oxidative and electrophilic stress induces multidrug resistance-associated protein transporters via the nuclear factor-E2-related factor-2 transcriptional pathway. *Hepatology.* **46**:1597–1610.
44. Tardif, J.C. 2003. Clinical results with AGI-1067: a novel antioxidant vascular protectant. *Am. J. Cardiol.* **91**:41A–49A.
45. Kamiya, K., et al. 2007. Phosphorylation of the cyclic AMP response element binding protein mediates transforming growth factor beta-induced downregulation of cyclin A in vascular smooth muscle cells. *Mol. Cell. Biol.* **27**:3489–3498.
46. Ichiki, T., et al. 2003. Cyclic AMP response element-binding protein mediates reactive oxygen species-induced c-fos expression. *Hypertension.* **42**:177–183.
47. Watson, P.A., Nesterova, A., Burant, C.F., Klemm, D.J., and Reusch, J.E. 2001. Diabetes-related changes in cAMP response element-binding protein content enhance smooth muscle cell proliferation and migration. *J. Biol. Chem.* **276**:46142–46150.
48. Pulver, R.A., Rose-Curtis, P., Roe, M.W., Wellman, G.C., and Lounsbury, K.M. 2004. Store-operated Ca2+ entry activates the CREB transcription factor in vascular smooth muscle. *Circ. Res.* **94**:1351–1358.
49. Lipskaia, L., et al. 2003. Phosphatidylinositol 3-kinase and calcium-activated transcription pathways are required for VLDL-induced smooth muscle cell proliferation. *Circ. Res.* **92**:1115–1122.
50. Guo, Y., et al. 2003. MRP8, ATP-binding cassette C11 (ABCC11), is a cyclic nucleotide efflux pump and a resistance factor for fluoropyrimidines 2′,3′-dideoxycytidine and 9′-(2′-phosphonylmethoxyethyl) adenine. *J. Biol. Chem.* **278**:29509–29514.
51. Dzau, V.J., Braun-Dullaeus, R.C., and Sedding, D.G. 2002. Vascular proliferation and atherosclerosis: new perspectives and therapeutic strategies. *Nat. Med.* **8**:1249–1256.
52. Novak, K. 1998. Cardiovascular disease increasing in developing countries. *Nat. Med.* **4**:989–990.
53. Humbert, M., Sitbon, O., and Simonneau, G. 2004. Treatment of pulmonary arterial hypertension. *N. Engl. J. Med.* **351**:1425–1436.
54. Leggas, M., et al. 2004. Mrp4 confers resistance to topotecan and protects the brain from chemotherapy. *Mol. Cell. Biol.* **24**:7612–7621.
55. Lum, H., et al. 1999. Expression of PKA inhibitor (PKI) gene abolishes cAMP-mediated protection to endothelial barrier dysfunction. *Am. J. Physiol.* **277**:C580–C588.
56. Lipskaia, L., et al. 2005. Sarco/endoplasmic reticulum Ca2+-ATPase gene transfer reduces vascular smooth muscle cell proliferation and neointima formation in the rat. *Circ. Res.* **97**:488–495.
57. Vallot, O., et al. 2000. Intracellular Ca(2+) handling in vascular smooth muscle cells is affected by proliferation. *Arterioscler. Thromb. Vasc. Biol.* **20**:1225–1235.